Analyzing the Impact of Distribution of Battery Energy Storage System for Participation in Frequency Regulation

Hassan Alsharif
Electrical and Biomedical Engineering
RMIT University
Melbourne, Australia
s3534091@student.rmit.edu.au

Mahdi Jalili
Electrical and Biomedical Engineering
RMIT University
Melbourne, Australia
mahdi.jalili@rmit.edu.au

Kazi N. Hasan
Electrical and Biomedical Engineering
RMIT University
Melbourne, Australia
kazi.hasan@rmit.edu.au

***Abstract*— The transition to low carbon energy systems requires more Renewable Energy Sources (RES) into the electricity grid. However, the high penetration of RESs may cause a significant reduction in the power system inertial response, which may adversely affect the frequency regulation. Many studies utilized the Battery Energy Storage System (BESS) to participate in frequency regulation services, where most of the research were using a large-scale BESS in one location. This paper presents an analysis to investigate the impact of the distribution of the BESS throughout the network on frequency regulation performance. The frequency responses of twenty different BESS allocation scenarios and under two different RES penetration levels have been compared, with the same aggregated BESS capacity, which is 100 MVA - just the total capacity has been distributed throughout the network. The simplified 14 generator South-Eastern Australian power system has been simulated by using DigSILENT/PowerFactory software. The simulation results have shown that the distribution of the BESS in multiple locations have demonstrated better frequency nadir. However, the improvement in the Rate of Change of Frequency (ROCOF) were dependent on the BESS locations.**

Keywords—Battery energy storage system, frequency stability, renewable generation, primary frequency control, power system inertia.

I. INTRODUCTION

Recently, the contribution of power generation from Renewable Energy Sources (RES) has increased noticeably, as might be inferred from stringent environmental protection rules, the reduced accessibility of fossil fuels, and the need to satisfy a raised global power demand [1]. Many countries have set their plans for replacing the conventional generators by RES. In Australia, some states are planning to increase the integration of RES in their power systems. For example, Victoria which aims to make 40% of its power generation comes from RES by 2025 [2], while South Australia has a massive target by making its power system 100% rely on RES by 2030 [3].

In a traditional power system, kinetic energy stored in the rotating parts of the Synchronous Generator (SG) is a significant property for frequency dynamics and stability. The contribution of inertia is a built-in feature of the SG where the rotating mass of the SG provides and absorbs the kinetic energy to/from the grid based on any frequency variations in the system [4]. In this manner, the SG maintains synchronism and prevents grid collapse or blackout.

In contrary, in modern power systems, most of the generation sources are integrated into the grid through power electronic converters. However, these new types of sources, e.g. RES do not support the power system inertia the same as what the conventional power generations do which make it challenging to maintain the frequency stability. Reducing the system inertia leads to increase the rate of change of frequency (ROCOF) and decrease the frequency nadir where this would have affected the overall power system stability and reliability [5].

Energy storage systems (ESS) with their fast-inertial response provide an excellent solution to support the frequency stability in low inertia power systems. In the literature, there are many types of energy storage systems that have been utilized to address the frequency stability challenges in converter-based power systems such as in [6]-[7]-[8]. Among all different types of ESS, BESS has been provided a promising solution with its continuous development related to the reduction in the investment cost and its ability in storing the energy with different capacities.

In [9], the role of a large-scale BESS in providing primary frequency control to a power system with high wind penetration level has been analyzed. The study has been tested in IEEE 9 buses and implemented in DigSILENT/PowerFactory software. The simulation results showed the ability of the BESS to reduce the system oscillations following the disturbance and support the incremental increase of RES penetration level. In [10], the ability of the BESS to participate in the frequency regulation services has been analyzed under various frequency events. A grid-scale BESS sizing strategy proposed in a modified IEEE-39 bus power system with a variety of scenarios using DigSILENT/PowerFactory [11]. The simulation results illustrated that the BESS successfully improved the frequency response and minimized the deviation in the power system frequency.

However, the previous strategies studied the role of large-scale BESS for frequency regulation support when they are placed just in one location. This approach utilizes a central controller to collect, process and distribute the information to respond to any imbalance in the power system which means that a vast communication infrastructure will be required. Also, in this approach the processing time form the BESS controller to response to any system imbalance is longer as the system information must go from/to only a central control system.

In contrary, the distributed approach of BESSs which relying on local information provides a good alternative. This approach does not only reduce the computation time which would be helpful for having a faster response but also accounts for system topology changes. Moreover, this strategy could take advantage of having local intelligent controllers that are able to communicate with each other to make smarter decisions [12]-[13]. Therefore, in this research an investigation has been conducted to analyze the impact of distributing the BESS on the system to provide frequency regulation support and compare that with having them only in one location. Twenty different distribution scenarios have been implemented where in each scenario, the same aggregated BESS capacity has been used. For the frequency regulation assessment, two frequency indices are adopted, i.e. frequency nadir, ROCOF (Rate of Change of Frequency).

II. POWER SYSTEM FREQUENCY STABILITY

In power system studies, the frequency stability can be defined as the ability of the power system to maintain the frequency within an acceptable level, i.e. normal operation frequency limit after a contingency event occurrence [14]. Typically, the contingency event causes an imbalance between the power system generation and load. Fig. 1 shows how the system frequency responds differently in high and low inertia power systems after the same contingency event.

In large power systems, frequency is not a global parameter and it varies among generators [15]. In a multimachine system, an equivalent generating unit is used to represent the average behavior of all synchronous units which known in the literature as Centre of Inertia (COI). According to [16], the COI frequency (f_{C}) can be calculated as in (1):

$$f_{C}\ (t) = \frac{\sum_{i=1}^{n} H_i S_{B-i} f_i(t)}{\sum_{i=1}^{n} H_i S_{B-i}} \quad (1)$$

where , S_{B-i} is the nominal apparent power of the generator in MVA, H_i is the inertia constant of the generator in seconds, $f_i(t)$ is the frequency response time of the *i-th* generator for a given time window.

A. Frequency Stability Indices

The frequency nadir and the Rate of Change of Frequency (ROCOF) are the most widely used indices for frequency response assessment [17]. The following subsections will briefly discuss these two frequency indicators.

1) Rate of Change of Frequency (ROCOF)

The ROCOF is the initial slope of the frequency change immediately following the contingency event and can be calculated using (1) [17]:

$$R\ (t) = \frac{d\ (t)}{d} \quad (2)$$

where f stands for frequency in Hz and $d\ (t)/d$ can be determined from the per-unit formulation of its swing equation as in (2) [17]:

$$\frac{d\ (t)}{d} = \frac{\frac{\Delta P(t)}{S_{B-i}}}{2H_i} f_0 = \frac{\frac{\Delta P(t)}{S_{B-i}}}{T_{N-i}} f_0 \quad (3)$$

where ΔP is the change of the active power in MW, T_{N-i} is the acceleration time constant in seconds, i refers to i_{th} generator among *n* generators in the system and f_0 is the nominal frequency in Hz.

The relationship between the stored kinetic energy E_{kin-I} in the rotating masses (MW·s) at nominal speed and the inertia constant H_i of n synchronous generators can be defined as in (4) where the total kinetic energy of the system can be calculated using (5) [17]. By substituting (4) into (3), we can get (6). An approximation of ROCOF that has been suggested in [18] in order to have a qualitative assessment for the frequency performance within a certain time window of the system inertia as in (7):

$$E_{k\ -i} = H_i \times S_{B-i} \quad (4)$$

$$E_{k\ -i} = \sum_{i=1}^{n} E_{k\ -i} \quad (5)$$

$$\frac{d\ (t)}{d} = \frac{\Delta P(t)}{2E_{k\ -i}} f_0 \quad (6)$$

$$R\ (t) = \frac{\Delta P_s\ (t)}{2(E_{k\ -s\ } - E_{k\ -i_0})} f_0 \quad (7)$$

Where *n* refers to the number of synchronous generators in the system, ΔP_{sys} and $E_{kin\text{-}lost}$ stand for the change in system active power and kinetic energy lost respectively due to a sudden disconnection of a generator.

2) Frequency nadir

The frequency nadir indicator represents the lower frequency value obtained after any power imbalance in the system and it depends on different factors in the power system, i.e. the system inertia, the frequency containment reserves, the setting of primary frequency control system, the location and size of the disturbance, and the pre-disturbance operating conditions [17]. This indicator has high relevance with the frequency control as a low frequency nadir value could lead to uncontrolled frequency excursions. The criterion that defines the minimum limit for frequency nadir can be expressed as ($f_n \gg f_m$), where f_m is the minimum acceptable frequency value which defined by grid operators.

III. BESS MODEL

In this section, the BESS model and all included models were developed in DigSILENT/PowerFactory and based on [19] are discussed. Fig. 2 illustrates the BESS structure used in this study. This BESS model includes a battery bank, a frequency controller, a charge controller, an active and reactive power controller, and a voltage source converter.

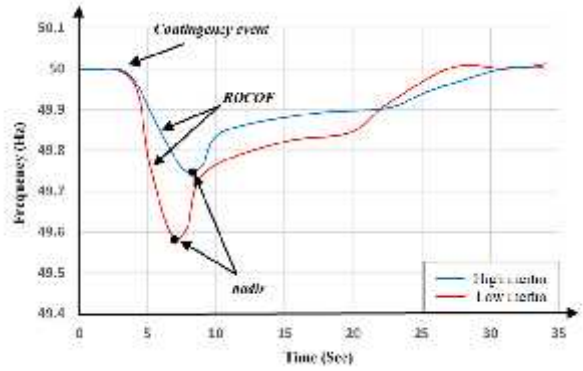

Fig. 1. Frequency nadir and ROCOF of high and low inertia power systems

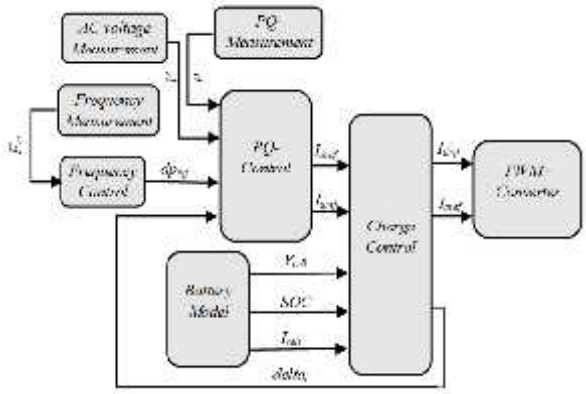

Fig. 2. BESS model

The models of each of these components will be discussed in the following subsections.

A. Battery model

In the battery model shown in Fig. 3, some assumptions are made to get a simple and at the same time functional model. At first, it is assumed that the battery is only discharged down to 20%. In that case, the voltage could be assumed as linearly dependent on the SOC. Furthermore, the internal resistance is assumed as constant and very small to be applicable for the high current application. The battery capacity is assumed as constant; thus, the expected capacity could be calculated and inserted in the model. Some other parameters in this model which are maximum cell voltage (V_{max}), minimum cell voltage (V_{min}), battery cell capacity (C_{bat}), internal resistance (R_i).

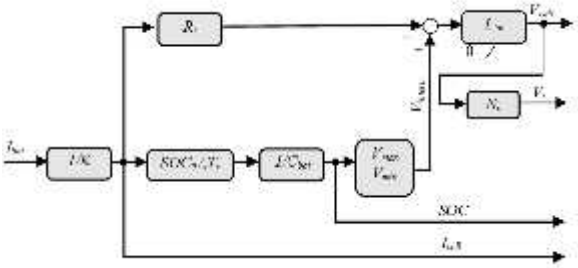

Fig. 3. Battery model

B. Frequency controller

The frequency controller uses a simple proportional controller with a small dead band as it is shown in Fig. 4. The droop defines how much active power is activated responding to any frequency deviation in the system. The full active power of the BESS is activated when the frequency deviation is equal to or greater than 2 Hz (in 50 Hz power systems). The block (*offset*) with the output (P_0) is used to compensate (dp_{ref}) if that value is not equal to zero after the load flow.

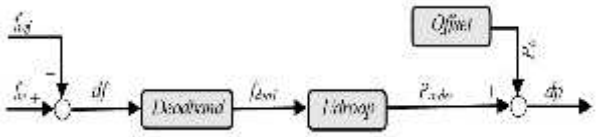

Fig. 4. Frequency controller

C. Charge controller

Fig. 5 shows the charge controller that has two main parts. First one is the charging logic which works to achieve the already described boundary conditions and the other part is the current limiter to limit the absolute value of the current order. In this controller, the active current has always a higher priority than the reactive current. In this model (Id_{ref_in}) refers to the difference of the reference current from the PQ-controller where (Id_{ref_out}) is the modified current from the charging logic.

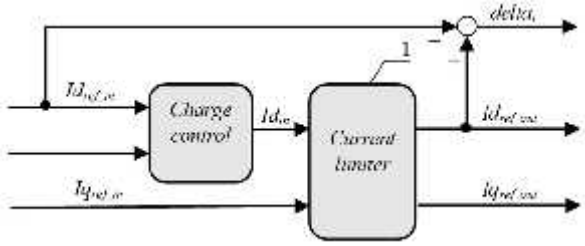

Fig. 5. Charge controller

D. Active and reactive power controller

This controller has two different paths, one for active power and the other for reactive power and they are controlled separately. In order to control the active power, the power first filtered in a first-order filter and added to the *deltai* that comes from the charge controller. The output deviation signal then used as an input for PI controller to define maximum (I_{d_max}) and minimum (I_{d_min}) active currents.

IV. Test System Model

The simplified 14-generator South-Eastern Australian power system model, that was developed by [20], was adopted in this study. This model contains different areas, which are Queensland (QLD), New South Wales (NSW), Victoria (VIC) including the Snowy Hydro (SH) and South Australia (SA), where Tasmania (TAS) was omitted. Some modifications were made to this model in order to align with the current and future trends, which have been done by [21] within DIgSILENT PowerFactory environment. In the modified model, a significant amount of additional generation was required to be added, as shown in Fig. 6, such as wind, solar photovoltaic (PV), hydro and battery energy storage (BES) where in total the system generation is equal to 14479.48 MW.

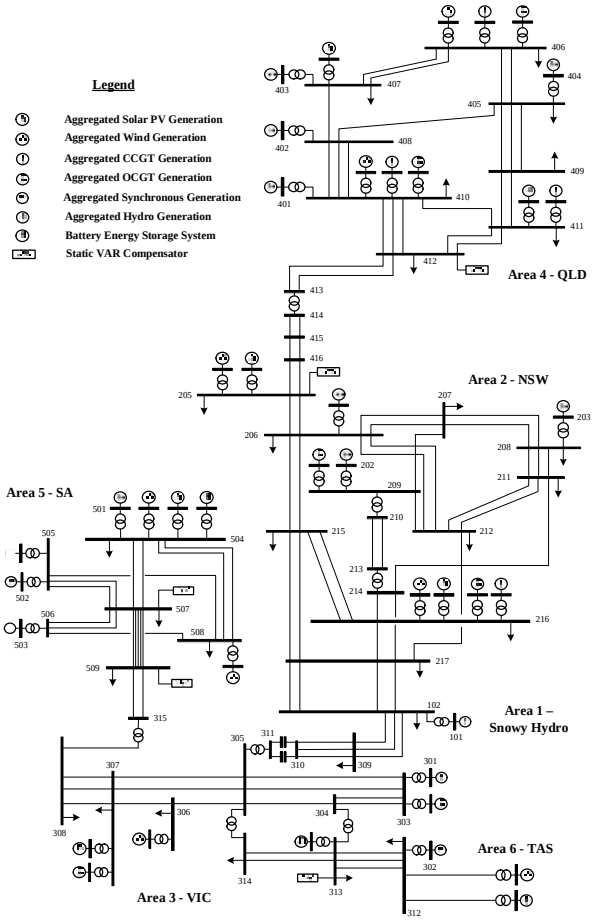

Fig. 6. Modified 14 generator South-Eastern Australian power system

In this study, the performance of BESS participation in frequency regulation services was investigated. Twenty distribution scenarios of the BESS in the system were analyzed under two penetration levels of RES where the BESS distributed among all Areas of the system. In each scenario, the same aggregated BESS capacity was utilized which equals to 100MW. For the frequency performance assessment, two frequency indicators were adopted, i.e. frequency nadir and ROCOF. The frequency event was created by considering the disconnection of the largest generation unit (which is 748MW in Area 4 – QLD). All simulations were implemented in DigSILENT/PowerFactory software which is a powerful tool in power system studies.

V. RESULTS AND DISCUSSION

Fig. 7 and Fig. 8 show the frequency nadir values of the system without using BESS and with BESS in twenty scenarios after the same contingency event under 35% and 55% RES penetration levels, respectively. For both 35% and 55% RES penetration levels, among all BESS distribution scenarios presented in Fig. 7 and Fig. 8, frequency nadir values were the best for placing the BESS in 3 locations. It can be seen for both cases that placing the BESS in one location got the worst nadir value compared with all other distribution scenarios. For both of these RES penetration levels, distributing the BESS in two and three locations were the best allocation scenarios among others (except the five locations scenario in 35% RES penetration) while the nadir values of the scenarios from 4 to 20 were very close from each other.

The ROCOF values that were obtained from the same scenarios are shown in Fig. 9 and Fig. 10 for 35% and 55% RES penetration levels respectively. In the ROCOF calculation of this study, a 500 ms time window following the contingency event was used. In 35% RES penetration level, by increase the BESS distribution, the ROCOF values were generally better than using only one location except for the two locations scenario. However, the ROCOF values were varying among the cases which make it hard to come up with a clear definition during this RES penetration level. When the RES penetration level increased to 55%, the ROCOF results of all scenarios can be classified into three patterns. First one is the best which happened when distributing the BESS in four to ten locations. The second pattern that gave the worst ROCOF values was by allocating the BESS all in eleven and twelve locations. The final one was the moderate pattern where the ROCOF values of the remained scenarios were relatively close.

Whereas the change in the frequency nadir and the ROCOF values after any system imbalance are highly dependent on the amount of the power system inertia, distribute the inertia support sources, i.e. BESS in multiple locations even with the same capacity seems to be able to make some difference in the frequency stability of the system. In both RES penetration levels, the improvement in the frequency nadir values was obvious when the BESS were distributed in multiple locations compared with placing them only in one location. This means that the time required from the BESS control systems to respond to any system imbalance is faster when they are allocated in different places in the system. However, the improvement in the ROCOF values appears to be cannot be obtained at any BESS distribution scenario. Thus, in order to have a such enhancement, the optimal locations of the BESS should be identified correctly.

VI. CONCLUSION AND FUTURE WORK

In this study, an analysis has been conducted to investigate how the distribution of the BESS in the network using the same capacity would impact on the frequency regulation performance of the power systems. For frequency performance assessment, the frequency nadir and ROCOF were used as frequency regulation indicators. Multiple BESS distribution scenarios under two RES penetration levels were simulated. The simulation results showed that the frequency nadir values has improved greatly by placing the BESS in multiple locations instead of one location in both RES penetration levels.

However, the ROCOF showed a slight improvement with generally unstable values by increasing the number of the locations in 35% RES penetration level. With 55% RES penetration level, increasing the distributions of the BESS led to the inconsistent ROCOF values, that is increased and decreased randomly. For further analysis, this study can be extended to find the optimal placement and sizing of the BESS and the impact of the contingency location on the BESS participation in frequency regulation services.

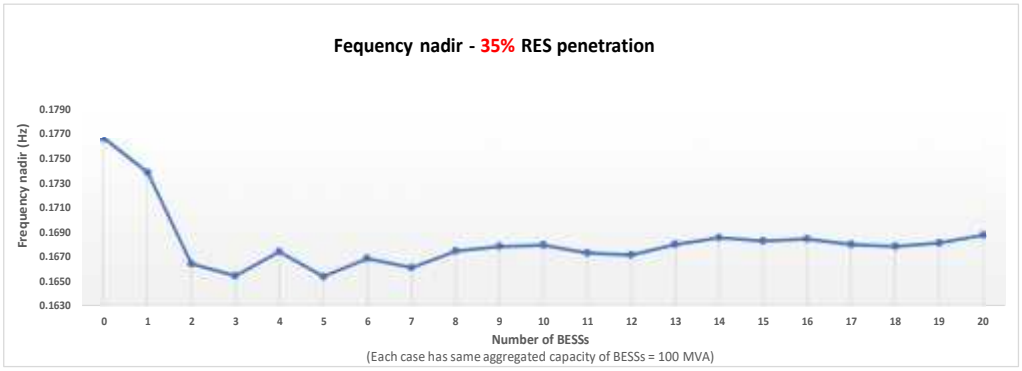

Fig. 7. Frequency nadir of 20 BESS distribution scenarios – 35% RES

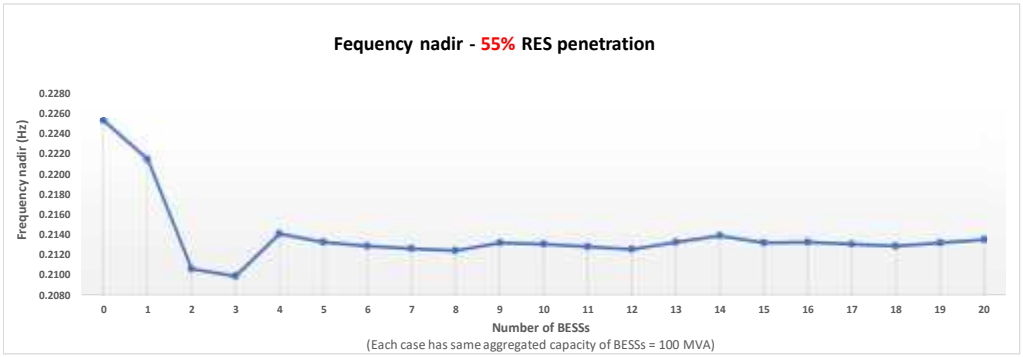

Fig. 8. Frequency nadir of 20 BESS distribution scenarios – 55% RES

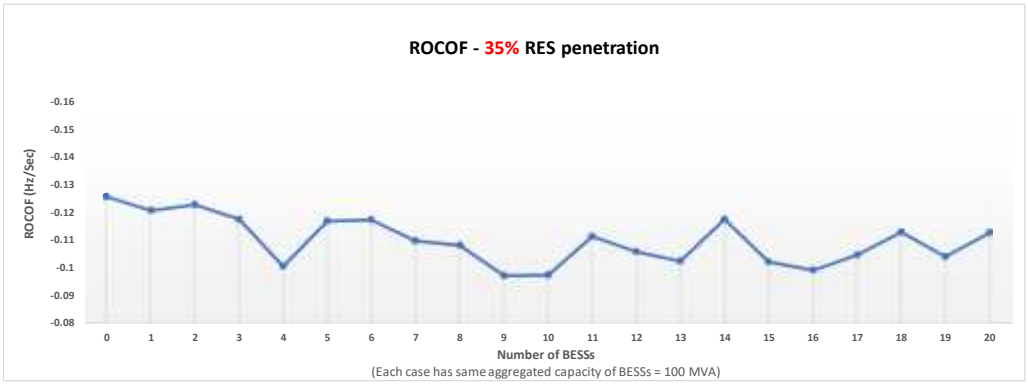

Fig. 9. ROCOF of 20 BESS distribution scenarios – 35% RES

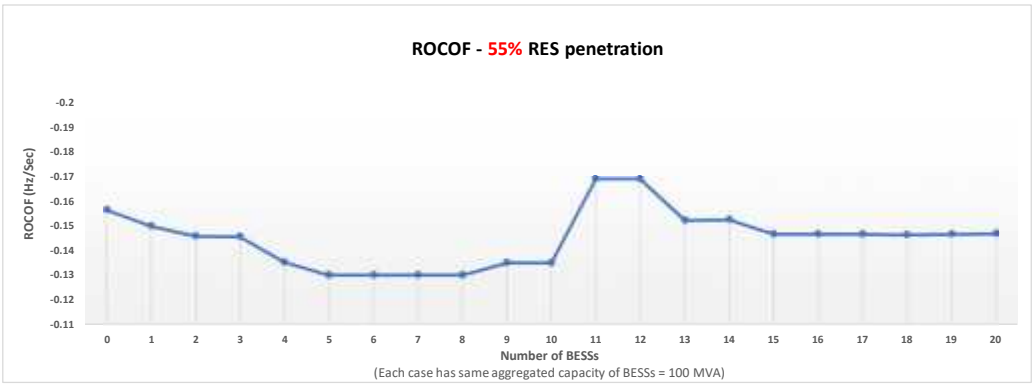

Fig. 10. ROCOF of 20 BESS distribution scenarios – 55% RES

REFERENCES

[1] A. Ulbig, T. S. Borsche, and G. Andersson, "Impact of Low Rotational Inertia on Power System Stability and Operation," *IFAC Proceedings Volumes*, vol. 47, no. 3, pp. 7290–7297, 2014, doi: 10.3182/20140824-6-za-1003.02615

[2] Victoria State Government, Renewable Energy Action Plan, [online], available: <https://www.energy.vic.gov.au/__data/assets/pdf_file/0014/74012/Web-pdf-RenewableEnergy-Action-Plan.pdf> [Accessed 17 October 2020].

[3] Clean Energy Australia Report, (2020), [online], available: <https://www.cleanenergycouncil.org.au/resources/resources-hub/clean-energy-australiareport> [Accessed 17 October 2020].

[4] M. Dreidy, H. Mokhlis, and S. Mekhilef, "Inertia response and frequency control techniques for renewable energy sources: A review," *Renewable and Sustainable Energy Reviews*, vol. 69, pp. 144–155, Mar. 2017, doi: 10.1016/j.rser.2016.11.170.

[5] Y. Wang, G. Delille, H. Bayem, X. Guillaud, and B. Francois, "High Wind Power Penetration in Isolated Power Systems—Assessment of Wind Inertial and Primary Frequency Responses," *IEEE Transactions on Power Systems*, vol. 28, no. 3, pp. 2412–2420, Aug. 2013, doi: 10.1109/tpwrs.2013.2240466.

[6] B. Cleary, A. Duffy, A. O'Connor, M. Conlon, and V. Fthenakis, "Assessing the Economic Benefits of Compressed Air Energy Storage for Mitigating Wind Curtailment," *IEEE Transactions on Sustainable Energy*, vol. 6, no. 3, pp. 1021–1028, Jul. 2015, doi: 10.1109/tste.2014.2376698.

[7] S. Rehman, L. M. Al-Hadhrami, and Md. M. Alam, "Pumped hydro energy storage system: A technological review," *Renewable and Sustainable Energy Reviews*, vol. 44, pp. 586–598, Apr. 2015, doi: 10.1016/j.rser.2014.12.040.

[8] C. Jauch and S. Hippel, "Hydraulic–pneumatic flywheel system in a wind turbine rotor for inertia control," *IET Renewable Power Generation*, vol. 10, no. 1, pp. 33–41, Jan. 2016, doi: 10.1049/iet-rpg.2015.0223.

[9] U. Datta, A. Kalam, and J. Shi, "The relevance of large-scale battery energy storage (BES) application in providing primary frequency control with increased wind energy penetration," *Journal of Energy Storage*, vol. 23, pp. 9–18, Jun. 2019, doi: 10.1016/j.est.2019.02.013.

[10] D. M. Greenwood, K. Y. Lim, C. Patsios, P. F. Lyons, Y. S. Lim, and P. C. Taylor, "Frequency response services designed for energy storage," *Applied Energy*, vol. 203, pp. 115–127, Oct. 2017, doi: 10.1016/j.apenergy.2017.06.046.

[11] C. K. Das *et al.*, "Optimal sizing of a utility-scale energy storage system in transmission networks to improve frequency response," *Journal of Energy Storage*, vol. 29, p. 101315, Jun. 2020, doi: 10.1016/j.est.2020.101315.

[12] T. Zhao and Z. Ding, "Distributed Agent Consensus-Based Optimal Resource Management for Microgrids," *IEEE Transactions on Sustainable Energy*, vol. 9, no. 1, pp. 443–452, Jan. 2018, doi: 10.1109/tste.2017.2740833.

[13] Y. Xu, W. Zhang, G. Hug, S. Kar, and Z. Li, "Cooperative Control of Distributed Energy Storage Systems in a Microgrid," *IEEE Transactions on Smart Grid*, vol. 6, no. 1, pp. 238–248, Jan. 2015, doi: 10.1109/tsg.2014.2354033.

[14] S. Impram, S. Varbak Nese, and B. Oral, "Challenges of renewable energy penetration on power system flexibility: A survey," *Energy Strategy Reviews*, vol. 31, p. 100539, Sep. 2020, doi: 10.1016/j.esr.2020.100539.

[15] K. N. Hasan and R. Preece, "Impact of Stochastic Dependence within Load and Non-synchronous Generation on Frequency Stability", *Bulk Power Systems Dynamics and Control Symposium* – IREP'2017, Espinho, Portugal, Aug. 27 – Sep. 1st, 2017.

[16] L. Ruttledge and D. Flynn, "Short-term frequency response of power systems with high non-synchronous penetration levels," *Wiley Interdisciplinary Reviews: Energy and Environment*, vol. 4, no. 5, pp. 452–470, Dec. 2014, doi: 10.1002/wene.158.

[17] E. Rakhshani, D. Gusain, V. Sewdien, J. L. Rueda Torres, and M. A. M. M. Van Der Meijden, "A Key Performance Indicator to Assess the Frequency Stability of Wind Generation Dominated Power System," *IEEE Access*, vol. 7, pp. 130957–130969, 2019, doi: 10.1109/access.2019.2940648.

[18] V. V. Terzija, "Adaptive Underfrequency Load Shedding Based on the Magnitude of the Disturbance Estimation," *IEEE Transactions on Power Systems*, vol. 21, no. 3, pp. 1260–1266, Aug. 2006, doi: 10.1109/tpwrs.2006.879315.

[19] U. Datta, A. Kalam, and J. Shi, "Battery Energy Storage System to Stabilize Transient Voltage and Frequency and Enhance Power Export Capability," *IEEE Transactions on Power Systems*, vol. 34, no. 3, pp. 1845–1857, May 2019, doi: 10.1109/tpwrs.2018.2879608.

[20] Gibbard M, Vowles D, "Simplified 14-generator model of the South East Australian power system," *The University of Adelaide, South Australia*. 2014 Feb 18:1-38.

[21] J. Bryant, P. Sokolowski, and L. Meegahapola, "Impact of FCAS Market Rules on Australia's National Electricity Market Dynamic Stability," *2019 IEEE International Conference on Industrial Technology (ICIT)*, Feb. 2019, doi: 10.1109/icit.2019.8755169.